A dedicated flavin-dependent monooxygenase catalyzes the hydroxylation of demethoxyubiquinone into ubiquinone (coenzyme Q) in Arabidopsis

Received for publication, July 9, 2021, and in revised form, September 30, 2021 Published, Papers in Press, October 6, 2021, https://doi.org/10.1016/j.jbc.2021.101283

Scott Latimer^{1,*}, Shea A. Keene², Lauren R. Stutts¹, Antoine Berger¹, Ann C. Bernert¹, Eric Soubeyrand¹, Janet Wright³, Catherine F. Clarke⁴, Anna K. Block⁵, Thomas A. Colquhoun², Christian Elowsky⁶, Alan Christensen³, Mark A. Wilson⁷, and Gilles J. Basset^{1,*}

From the ¹Department of Horticultural Sciences and ²Department of Environmental Horticulture, Plant Innovation Center, Institute of Food and Agricultural Sciences, University of Florida, Gainesville, Florida, USA; ³School of Biological Sciences, University of Nebraska-Lincoln, Lincoln, Nebraska, USA; ⁴Department of Chemistry and Biochemistry and the Molecular Biology Institute, University of California, Los Angeles, California, USA; ⁵Center for Medical, Agricultural and Veterinary Entomology, Chemistry Research Unit, ARS, USDA, Gainesville, Florida, USA; ⁶Department of Agronomy and Horticulture and ⁷Department of Biochemistry and Redox Biology Center, University of Nebraska-Lincoln, Lincoln, Nebraska, USA

Edited by Joseph Jez

Ubiquinone (Coenzyme Q) is a vital respiratory cofactor and liposoluble antioxidant. In plants, it is not known how the C-6 hydroxylation of demethoxyubiquinone, the penultimate step in ubiquinone biosynthesis, is catalyzed. combination of cross-species gene network modeling along with mining of embryo-defective mutant databases of Arabidopsis thaliana identified the embryo lethal locus EMB2421 (At1g24340) as a top candidate for the missing plant demethoxyubiquinone hydroxylase. In marked contrast with prototypical eukaryotic demethoxyubiquinone hydroxylases, the catalytic mechanism of which depends on a carboxylatebridged di-iron domain, At1g24340 is homologous to FADdependent oxidoreductases that instead use NAD(P)H as an electron donor. Complementation assays in Saccharomyces cerevisiae and Escherichia coli demonstrated that At1g24340 encodes a functional demethoxyubiquinone hydroxylase and that the enzyme displays strict specificity for the C-6 position of the benzoquinone ring. Laser-scanning confocal microscopy also showed that GFP-tagged At1g24340 is targeted to mitochondria. Silencing of At1g24340 resulted in 40 to 74% decrease in ubiquinone content and de novo ubiquinone biosynthesis. Consistent with the role of At1g24340 as a benzenoid ring modification enzyme, this metabolic blockage could be bypassed by supplementation 4-hydroxybenzoate, the immediate precursor of ubiquinone's ring. Unlike in yeast, in Arabidopsis overexpression of demethoxyubiquinone hydroxylase did not boost ubiquinone content. Phylogenetic reconstructions indicated that plant demethoxyubiquinone hydroxylase is most closely related to prokaryotic monooxygenases that act on halogenated aromatics and likely descends from an event of horizontal gene transfer between a green alga and a bacterium.

Ubiquinone is made up of prenyl and benzoquinone moieties (Fig. 1). In flowering plants, the early ubiquinone precursors are mevalonate for the prenyl chain and phenylalanine and tyrosine for the benzenoid ring (11-14). In Arabidopsis thaliana, phenylalanine is the preferred ring precursor and is incorporated into ubiquinone via the formation of 4-hydroxybenzoate (12–14). Arabidopsis genes for the prenylation of 4-hydroxybenzoate, as well as for the O- and C-methylations and C5-hydroxylation of the ring, have been identified (4, 15, 16). The subcellular localization of the prenyltransferase and the O-methyltransferase has been investigated, and both enzymes have been shown to be mitochondrial (4, 15). By contrast, nothing is known in plants about the other ring decoration steps, including decarboxylation and hydroxylation at the C-1 position and hydroxylation at the C-6 position. The C6-hydroxylation, which represents penultimate step in ubiquinone biosynthesis, is of specific interest because it has been shown in other eukaryotes to control the flux of ubiquinone production and to be subjected to posttranslational regulations (17-19). In metazoans, yeast, and some bacteria, the corresponding enzyme is an O₂-dependent carboxylate-bridged diiron protein called Coq7 (EC 1.14.99.60; Fig. 1), also known as clk-1 or CAT5, which uses

^{*} For correspondence: Gilles Basset; Scott Latimer, scottlatimer@ufl.edu.



Ubiquinone (Coenzyme Q) is a liposoluble redox cofactor that fulfills vital functions both as an electron carrier of the respiratory chain and as a component of the antioxidant machinery of the cell (1, 2). Reflecting such core functions, genetic defects that fully block ubiquinone biosynthesis in plants result in embryo lethal phenotypes (3, 4). Because ubiquinone is one of the major liposoluble free-radical scavengers in eukaryotes (1, 5), there has been sustained interest in engineering crops with higher ubiquinone content in order to enhance their nutritional value and improve their resistance to abiotic stresses (6–10). This engineering approach, however, is contingent upon the knowledge of the ubiquinone biosynthetic pathway and its regulation in plants.

Figure 1. Structure of ubiquinone and nomenclature of the hydroxy-lases associated to its biosynthesis. UbiF, UbiI, UbiH, and Coq6 are FAD-dependent monooxygenases; Coq7 is an unrelated carboxylate-bridged diiron protein. Some bacteria possess multifunctional hydroxy-lases, some of which specifically induced in anaerobiosis or microaerobiosis, which are not represented here. Question marks indicate that the corresponding hydroxylase is unknown. The letter n designates the number of isoprenyl units (C5) in the polyprenyl moiety of ubiquinone. This number can vary between species; for instance, ubiquinone-6, ubiquinone-8 and ubiquinone-9 are the predominant forms in Saccharomyces cerevisiae, Escherichia coli, and Arabidopsis thaliana, respectively.

demethoxyubiquinone as a cosubstrate (20-23). Land plants and green algae lack homologs of this enzyme. Escherichia coli does not possess a Coq7 homolog either, but has instead a catalytically equivalent—though structurally unrelated—FADdependent monooxygenase called UbiF (Fig. 1; (24)). E. coli also has two additional FAD-dependent monooxygenases, called UbiH (EC 1.14.99.B5) and UbiI (EC 1.14.13.240), which catalyze the C-1 and C-5 hydroxylations, respectively (25, 26). However, this framework of dedicated monooxygenases for each reaction of hydroxylation in ubiquinone biosynthesis is not universal as many bacteria have evolved enzymes that catalyze more than one hydroxylation on the benzenoid ring; these include atypical O₂-independent hydroxylases as well as bifunctional (C-1/C-5 hydroxylations) or even trifunctional (C-1/C-5/C-6 hydroxylations) FAD-dependent monooxygenases (23, 27). Such an evolutionary precedent for the of nonregioselective FAD-dependent monoexistence oxygenases is significant because Arabidopsis encodes an FAD-dependent monooxygenase, COO6 (At3g24200), which complements a yeast ubiquinone biosynthetic mutant lacking C-5 hydroxylase activity (Fig. 1; (16)). Given the absence of Coq7 homologs in plants, the question arises as to whether this Arabidopsis COQ6 could also hydroxylate the C-1 and C-6 ring positions.

The identification of plant ubiquinone biosynthetic genes corresponding to the ring decoration steps has historically been achieved via homology searches and complementation of cognate null mutants in yeast (4, 15, 16). Yet, applying this strategy to search for the missing plant C-6 hydroxylase is not straightforward. Indeed, not only are COQ7 homologs absent from plant genomes, but in yeast the presence of the Coq7 protein is required for the stability of other enzymes and proteins involved in ubiquinone biosynthesis (28). Because the missing plant C-6 hydroxylase is necessarily a non-Coq7 homolog, it appears unlikely that this enzyme would meet the structural requirements for the functional replacement of Coq7 in yeast complementation assays.

In this study, we deploy parallel complementation strategies designed to mitigate the shortcomings of structural compatibility between plant monooxygenase candidates and the hydroxylation of demethoxyubiquinone in yeast and E. coli. Having shown that Arabidopsis COQ6 behaves as a strict C-5 hydroxylase in complementation assays, we combine phenotypic and gene coexpression data mining to identify the authentic plant demethoxyubiquinone hydroxylase.

Results

Arabidopsis COQ6 is a monofunctional flavin-dependent monooxygenase

To determine whether the Arabidopsis FAD-dependent COQ6 monooxygenase doubles as the enzyme responsible for the hydroxylation at the C-6 position of ubiquinone's ring, its full-length cDNA was subcloned into yeast expression vector pYES-DEST52 and introduced into yeast strain E194KCoq7. This strain harbors a missense mutation that affects the diiron center of Coq7; the E194KCoq7 cells therefore lack Coq7 activity and are devoid of ubiquinone (28). Unlike the coq7 null mutant, however, the E194KCoq7 strain still produces the coq7 polypeptide, which despite being catalytically inactive retains the capacity to stabilize other ubiquinone biosynthetic proteins (28). Such an arrangement is notable as it allows the E194KCoq7 mutant to accumulate demethoxyubiquinone, the substrate of the Coq7-catalyzed reaction, and facilitates functional complementation by structurally unrelated FAD-dependent monooxygenases (28). Yet, HPLC analyses showed that the extract of E194KCoq7 cells expressing Arabidopsis COQ6 did not contain detectable amount of ubiquinone (Fig. 2A). As expected, no complementation was observed in the cells harboring empty pYES-DEST52, while expression of wild-type Coq7 restored ubiquinone biosynthesis (Fig. 2A).

To confirm these results, the Arabidopsis COQ6 cDNA was cloned without its targeting presequence-encoding region into expression vector pBAD24 and introduced into the E. coli null mutants corresponding to FAD-dependent monooxygenases UbiI, UbiH, and UbiF. As expected here again, HPLC analyses of bacterial extracts indicated that expression of Arabidopsis COO6 in the AubiIc mutant resulted in the restoration of ubiquinone production and near complete disappearance of the early ubiquinone biosynthetic intermediate, octaprenyl phenol (Fig. 2B). In contrast, either marginal or no restoration of ubiquinone production was observed for the ΔubiH and ΔubiF null mutants, respectively (Fig. 2, C and D). Together these results demonstrate that Arabidopsis COQ6 does not moonlight as a demethoxyubiquinone hydroxylase, and therefore that plants must possess a separate enzyme to catalyze the hydroxylation at the C-6 position of the benzoquinone ring.

Plants have flavin-dependent oxidoreductases of unknown function that are essential for embryo development and are coexpressed with respiratory genes

We hypothesized that the gene encoding plant demethoxyubiquinone hydroxylase should fit the criteria classically

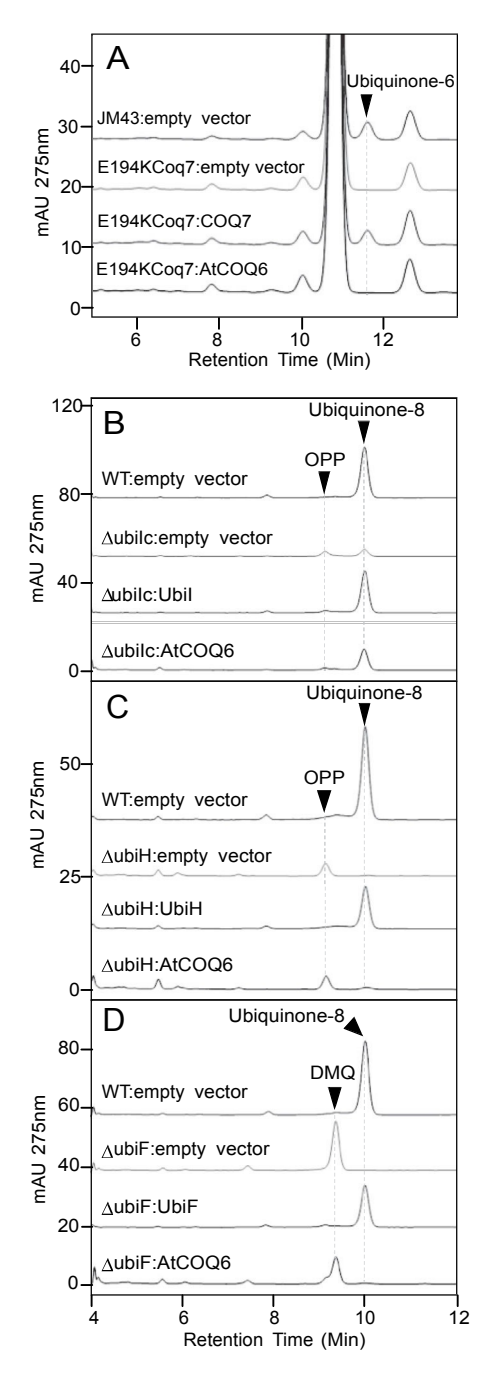


Figure 2. AtCOQ6 functions as a strict C-5 monooxygenase. A, ubiquinone analyses in wild-type (JM43) and E194KCoq7 yeast cells. Extracts were obtained from similar number of cells grown in minimal medium containing 0.1% glucose (w/v) and 2% (w/v) D-galactose and harvested in exponential phase of culture. Extracts were analyzed by HPLC with diode array detection. B-D, ubiquinone analyses in E. coli. Cells were grown on LB medium with 0.02% arabinose as an inducer, except for the AtCOQ6 construct-bearing strains that were induced with 0.2% arabinose and the ΔubiF:UbiF strain that was grown without inducer. Extracts from identical number of cells were analyzed by HPLC with diode array detection. ΔubiIc designates a ΔubiI strain that has been cured of its original deletion cassette; this strain contains trace amounts of ubiquinone owing to the C-5 hydroxylase moonlighting activity of UbiF (26). DMQ, demethoxyubiquinone; OPP, 2-octaprenylphenol.

observed for ubiquinone biosynthetic genes: i) its loss of function should result in the absence of ubiquinone and therefore cause embryo lethality, and ii) its coexpression

network should display some functional connections with the respiratory chain. Searching a recently updated dataset of known embryo-defective mutants (510 genes) in Arabidopsis (29) using the term "hydroxylase" identified a single entry, EMB2421 (At1g24340), annotated as "polyketide hydroxylaserelated monooxygenase." Neither At1g24340 nor any of its plant orthologs have a known cellular function. Since the EMB2421 locus was identified via a single untagged T-DNA insertion (30), two additional T-DNA lines corresponding to independent insertions in At1g24340's first (SALK 073461C and SALK 084134) were examined. For both lines about 25% of the segregating seeds in the siliques of the self-pollinated heterozygous plants were indeed aborted and no homozygous mutant could be recovered (Fig. S1). Crossspecies analyses of the coexpression profiles of At1g24340 and its orthologs in Medicago, soybean, rice, and tomato indicated that a number of respiratory genes were repeatedly detected among the top 0.8 to 1.2% expressed loci of each cognate database (Fig. 3A; Dataset S1). Most remarkable among these tightly coregulated genes were ubiquinone biosynthetic genes themselves, including COQ6 (soybean, Medicago, rice), COQ9 (Arabidopsis, Tomato, rice), COQ8 (Arabidopsis, Medicago), COQ10 (soybean), COQ5 (Tomato), COQ3 and COQ1 (rice) (Fig. 3A). We consequently deemed At 1g24340 as a strong candidate for the missing plant demethoxyubiquinone hydroxylase.

At1g24340 encodes for a 709 amino acid protein (rv78 kDa) that possesses a conserved FAD/NAD(P)H binding domain (InterPro 002938; residues 47-421) (Fig. 3, B and C). This domain is found in a number of FAD-dependent oxidoreductases that use NAD(P)H as an electron donor and O2 as a cosubstrate, including the UbiF/UbiH/UbiI/COQ6 monooxygenases (Fig. 3, B and C). At1g24340, however, markedly differs from these proteins in that it features an additional unintegrated region (residues 518-709) resulting in a protein that is 23 to 36 kDa larger than these other monooxygenases (Fig. 3, B and C). Structure modeling predicted At 1g24340's unintegrated region folds as a thioredoxin domain (Fig. 3C); the latter, however, lacks the canonical CXXC motif. The closest At1g24340 homologs of known function are bacterial hydroxylases involved in the catabolism of halogenated aromatic compounds; we will return to this topic later.

At1g24340 is targeted to mitochondria

At1g24340 and its orthologs sampled among vascular plants display highly divergent N-terminal extensions of 22 to 48 residues that are characteristic of organelle targeting sequences (Fig. 4A). DeepLoc-1.0 (31) and Predotar (32) analyses gave high probability (>80%) for localization of At1g24340 to the mitochondrion (Table S1), and a high-throughput proteomics study detected At1g24340's signature peptides in purified leaf mitochondria (33). In contrast, the output of a Wolf Psort (34) analysis indicated that ten of At1g24340's top 14 nearest neighbors were localized in the chloroplast, one was cytosolic, and only three were mitochondrial (Table S1). IPSORT predicted At1g24340 as having a chloroplast transit

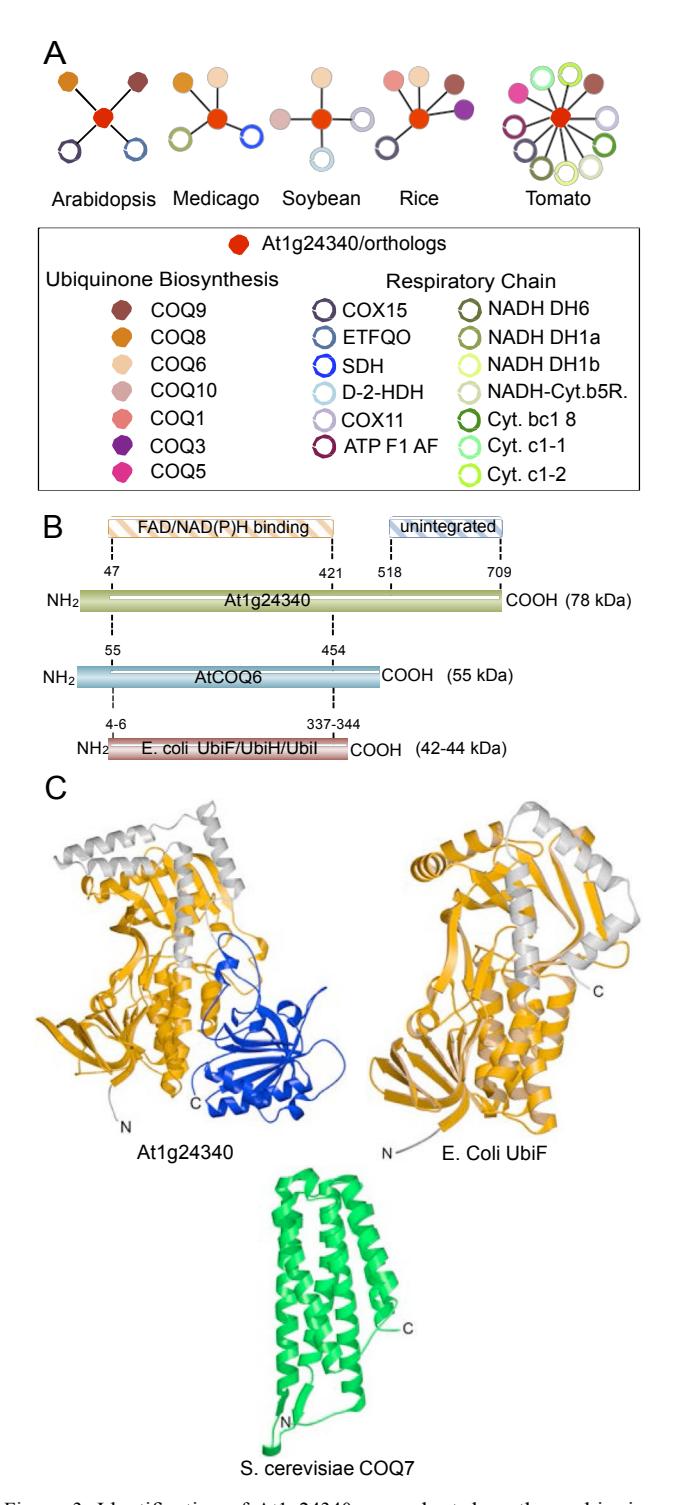


Figure 3. Identification of At1g24340 as a plant demethoxyubiquinone hydroxylase candidate. A, reconstructed functional networks of At1g24340 and its orthologs in Medicago truncatula, soybean, rice, and tomato. Known respiratory genes were extracted from the top 200 coexpressors of At1g24340 and its orthologs using the ATTED-II database. The 200 coexpressor cutoff represented 0.9%, 1%, 1.2%, 0.8%, and 1% of the total expressed loci available for Arabidopsis, Medicago truncatula, soybean, rice, and tomato, respectively. The ranked and annotated lists of these genes as well as gene abbreviations are provided in Dataset S1. Full color circles represent ubiquinone biosynthetic genes (COQ); open circles represent genes encoding for components of the respiratory chain or for redox enzymes directly connected to it. Identical colors indicate orthology between species. B, schemes comparing the domain organization and size of At1g24340 with those of Arabidopsis COQ6 (AtCOQ6) and E. coli monooxygenases UbiF, UbiH, and UbiI. Numbers indicate the beginning and end

peptide (Table S1). To disambiguate the subcellular localization of At1g24340, its full-length cDNA—minus its stop codon (Table S2)—was fused in-frame to the 50-end of GFP, and this construct was coinfiltrated with an RFP-tagged mitochondrial marker in Nicotiana benthamiana epidermal cells. Laser-scanning confocal microscopy showed that both fluorescent reporter proteins imaged as discrete punctate structures that moved quickly along cytosolic streams as typically observed for mitochondria (Fig. 4, B, C, and E). Strict overlap of the GFP and RFP signals was observed in cells that coexpressed the corresponding fusion proteins, while no GFP-associated fluorescence was observed in plastids (Fig. 4, D and E). At1g24340 appears therefore to be targeted exclusively to mitochondria.

At1g24340 complements the C-6 hydroxylation defect of the yeast E194KCoq7 and E. coli ΔubiF knockouts

Expression of At1g24340's full-length cDNA into the yeast E194KCoq7 point mutant restored the ability of these cells to utilize nonfermentable carbon substrates, and the growth of this transformant was similar to that of the E194KCoq7 mutant after reintroduction of a functional Coq7 copy (Fig. 5A). Furthermore, HPLC analyses confirmed that ubiquinone-6 biosynthesis had been restored E194KCoq7 cells harboring the At1g24340 construct (Fig. 5B). Similarly, expression of a matured version of At1g24340—i.e., minus its mitochondrial presequence—complemented an E. coli ΔubiF mutant strain, both when scored for restoration of ubiquinone-8 production and decrease in the accumulation of demethoxyubiquinone-8, the substrate of UbiF (Fig. 5C). In contrast, no complementation was observed when At1g24340 was expressed in the ΔubiIc and ΔubiH mutant strains (Fig. 5, D and E). These data demonstrate that At1g24340 bears demethoxyubiquinone hydroxylase activity and that this enzyme displays strict specificity for the C-6 position of the benzoquinone ring.

At1g24340 knockdown plants display impaired ubiquinone biosynthesis, while overexpression of At1g24340 does not boost ubiquinone level in Arabidopsis

To circumvent the embryo lethal phenotype associated with the complete blockage of ubiquinone biosynthesis in plants and directly investigate the function of At1g24340 in Arabidopsis, antisense constructs constitutively targeting three regions of At1g24340's mRNA were generated (Fig. 6A). Transformants were recovered for all three constructs. Realtime quantitative RT-PCR analysis performed on T1 plants identified five lines (3–10, 3–12, 2–4, 1–3, and 2–1) with

residues of predicted FAD/NAD(P)H binding domains (orange stripes) or unintegrated domain (blue stripes). C, Alphafold-generated ribbon diagrams of demethoxyubiquinone hydroxylase At1g24340, E. coli UbiF, and S. cerevisiae COQ7. The FAD/NAD(P)H binding domains of the Arabidopsis and E. coli proteins are shown in the same orientation and are colored in orange. The C-terminal unintegrated domain with similarity to thioredoxin in the Arabidopsis protein is shown in blue. Domain boundaries are the same as indicated in B. The structurally unrelated S. cerevisiae COQ7 is shown in green. The predicted targeting presequences of At1g24340 and S. cerevisiae COQ7 (rv40 amino acids) were disordered in the corresponding Alphafold models and have been removed for clarity.

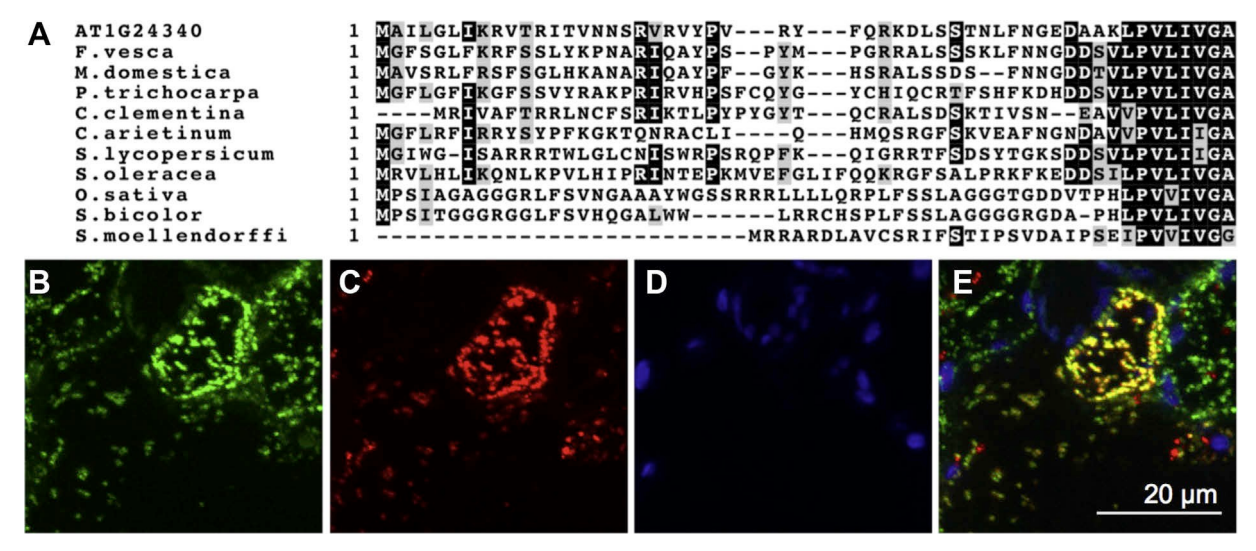


Figure 4. Subcellular localization of At1g24340. A, alignment of the N-terminal regions of At1g24340 and its orthologs in Fragaria vesca, Malus domestica, Populus trichocarpa, Citrus clementina, Cicer arietinum, Solanum lycopersicum, Spinacia oleracea, Oryza sativa, Sorghum bicolor, and Selaginella moellendorffii. Identical and similar residues are shaded in black and gray, respectively. Dashes represent gaps introduced to maximize alignment. B, transient expression and confocal microscopy imaging of At1g24340 fused to the N-terminus of GFP in Nicotiana benthamiana epidermal cells. C, RFP-tagged isovaleryl-CoA dehydrogenase (mitochondrial marker). D, auto-fluorescence of chlorophyll. E, overlay of the green, red, and blue pseudo-colors.

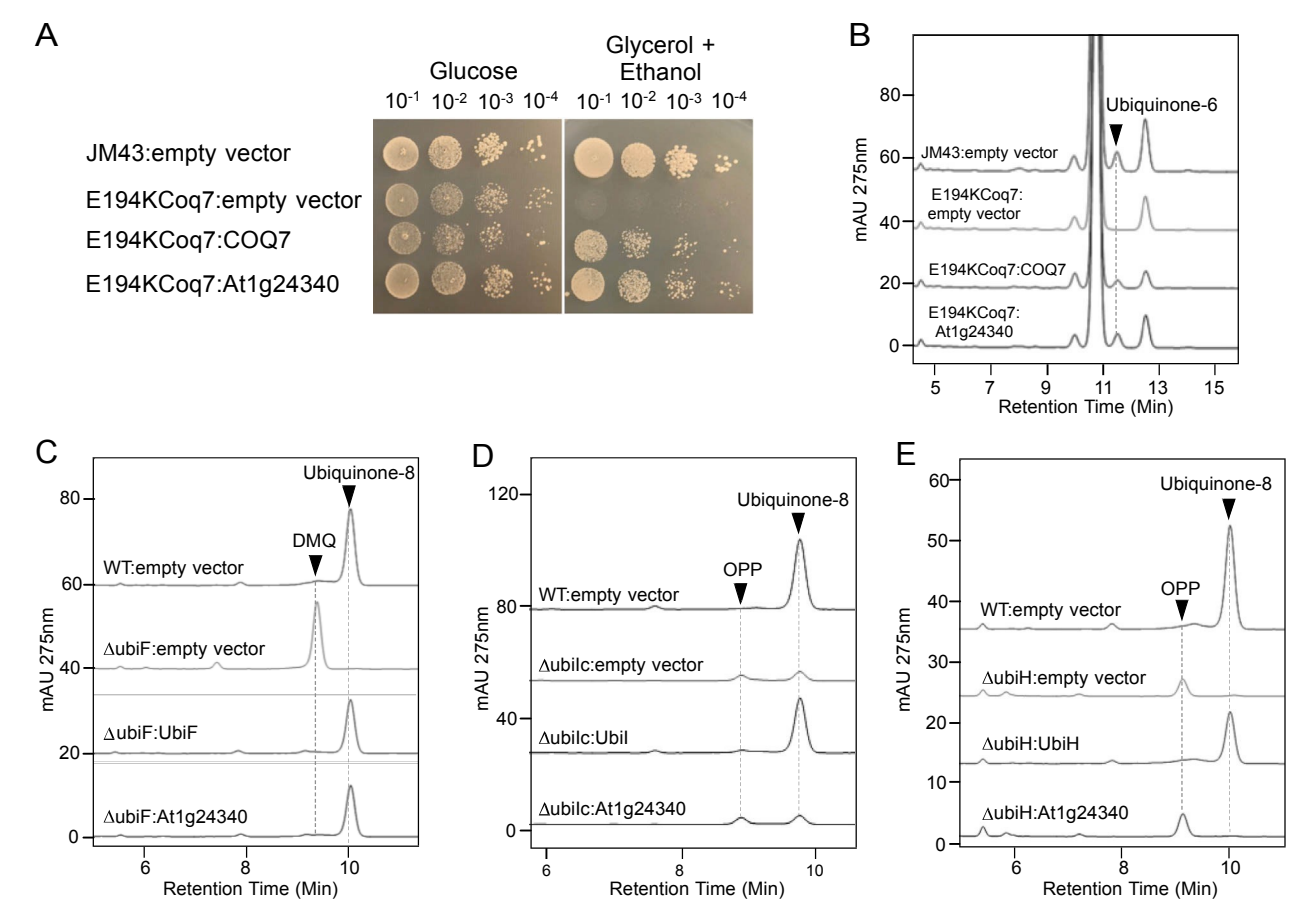


Figure 5. At1g24340 complements the yeast E194KCoq7 and E. coli ΔubiF Knockouts. A, functional complementation of yeast E194Kcoq7 point mutant. Dilutions of identical number of cells were spotted on solid minimal medium containing 2% (w/v) glucose (fermentable) or 3% (v/v) glycerol/2.5% (v/v) ethanol (nonfermentable) as carbon sources and 0.05% (w/v) D-galactose as an inducer. JM43 is the wild-type parent strain of E194Kcoq7. B, ubiquinone analyses in wild-type and E194KCoq7 yeast cells. Extracts were obtained from similar number of cells grown in minimal medium containing 0.1% glucose (w/v) and 2% (w/v) D-galactose and harvested in exponential phase of culture. Extracts were analyzed by HPLC with diode array detection. C–E, ubiquinone analyses in E. coli. Extracts from identical number of cells were analyzed by HPLC with diode array detection. DMQ, demethoxyubiquinone; OPP, 2-octaprenylphenol.

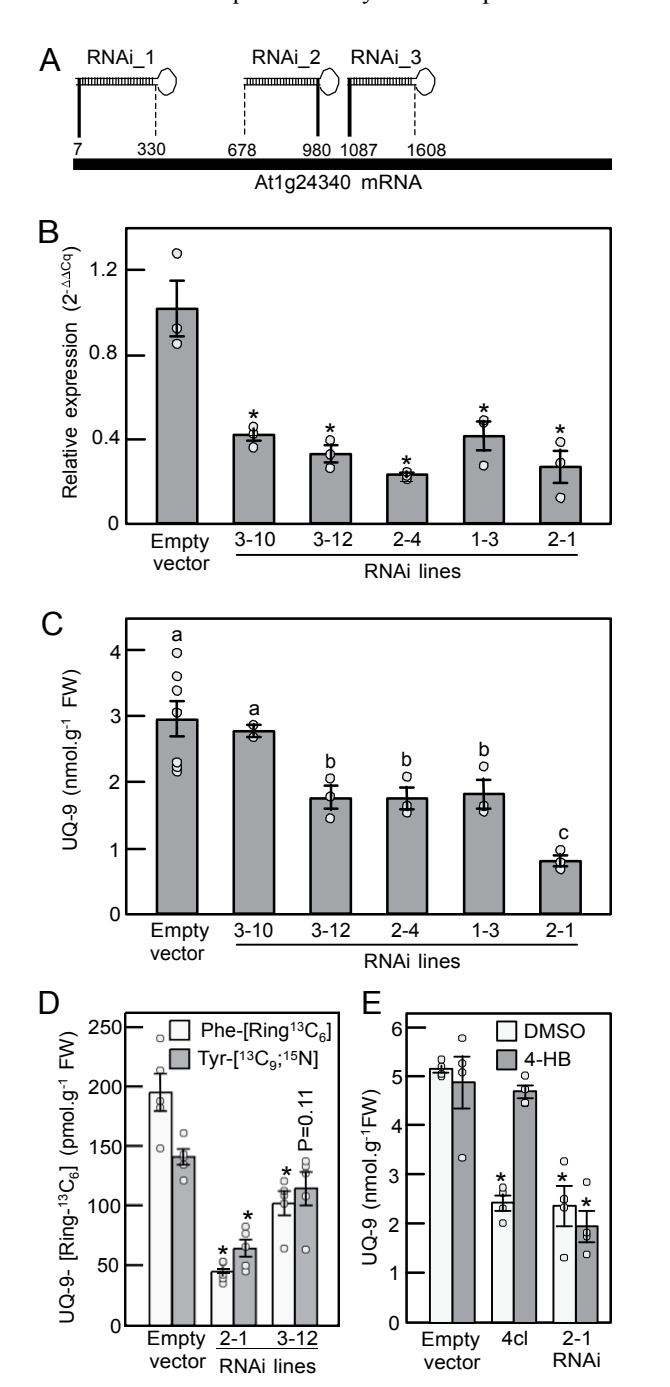


Figure 6. Silencing of At1g24340. A, scheme showing the location of RNAi constructs 1, 2, and 3. B, qRT-PCR analyses of At1g24340 mRNA levels in the rosette leaves of T1 plants corresponding to empty-vector control lines and silenced transgenics from lines 3-10, 3-12, 2-4, 1-3, and 2-1. Each transgenic line originates from an independent event of insertion. Data are means of three biological replicates ±SE. Single asterisks indicate significant differences from the empty-vector control as determined by Fisher's test $(p < \alpha = 0.05)$ from an analysis of variance. C, total ubiquinone-9 content in the rosette leaves of 4-week-old empty vector control plants and silenced transgenics from lines 3–10, 3–12, 2–4, 1–3, and 2–1. Data are means of 7 (empty vector) to 3 (RNAi plants 3–12, 2–4, 1–3, and 2–1) or 2 (RNAi plants 3–10) biological replicates \pm SE. Columns with differing letter annotations are significantly different from each other as determined by Fisher's test (p < α = 0.05) from an analysis of variance. D, ubiquinone-9-[Ring- 13 C₆] content in axenically grown homozygous T3 seedlings corresponding to empty-vector control, and RNAi lines 2–1 and 3–12. Plants were fed for 3 h with 250 μ M of Phe-[Ring- $^{13}C_6$] or Tyr-[$^{13}C_9$, ^{15}N]. Data are means of five biological replicates ±SE. Single asterisks indicate significant differences from the corresponding empty-vector control (i.e., Phe fed or Tyr fed) as determined by Fisher's test (p < α = 0.05) from an analysis of variance. E, total

pronounced decreases in the level of At1g24340 transcripts, the value of which ranged from 23% to 41% of that of the vector alone controls (Fig. 6B). HPLC analyses of rosette leaf extracts indicated that the ubiquinone-9 content of these transgenics was 40% (RNAi plants 1-3, 2-4, 3-12) to 74% (RNAi plant 2-1) lower than that measured for the vector alone control (Fig. 6C). Similar marked decreases were observed for the isotopic enrichment of ubiquinone-9 when either of the early precursors of its benzenoid ring, Phe-[Ring-¹³C₆] and Tyr-[¹³C₉; ¹⁵N], was fed to axenic cultures of RNAi plants 2-1 and 3-12 (Fig. 6D). Furthermore, in contrast to the situation observed for a p-coumaroyl-CoA ligase (4 cl) which is impaired in the formation of 4-hydroxybenzoate (12), feeding this immediate precursor of ubiquinone's ring did not restore ubiquinone level in RNAi plants 2-1 (Fig. 6E). All together these results demonstrate that the loss of function of At1g24340 results in a metabolic blockage downstream of the formation of ubiquinone's ring and confirm that At1g24340 acts as a ring modification enzyme. As previously observed for Arabidopsis mutants displaying similar losses in ubiquinone content (12, 14), At1g24340 silenced plants were visually indistinguishable from their wild-type parent (data not shown).

In parallel, Arabidopsis lines overexpressing At1g24340 cDNA under the control of the constitutive 35S promoter were generated. Real-time quantitative RT-PCR analysis showed that in homozygous T3 overexpressor lines 9–5, 11–2, and 16–1, the levels of At1g24340 transcripts were 28, 15, and 20 times higher than that of the empty vector controls, respectively (Fig. 7A). None of these lines, however, displayed any statistically significant increase in ubiquinone content as compared with their empty vector counterparts (Fig. 7B).

At1g24340 is closely related to bacterial FAD-dependent monooxygenases involved in the catabolism of halogenated aromatic compounds

BLAST searches of the NCBI database using At1g24340 as a query detected orthologs throughout green plant lineages except Gymnosperms (Fig. 8A). These orthologs appeared to be also absent in Glaucophytes and Rhodophytes, the latter having Coq7 homologs such as yeast and metazoans (Fig. 8A). Close homologs of At1g24340 (25–31% identity) were nonetheless detected outside the Archaeplastida clade, including in bacteria, fungi, and unsurprisingly in the secondary plastid-bearing Cryptomonads (Fig. 8A). Notable among these nonplant homologs are bacterial FAD-dependent monooxygenases that operate in the degradation pathway of halogenated aromatic compounds and that display the same substrate regioselectivity as At1g24340 (Fig. 8, A and B; (35, 36)). The

ubiquinone-9 content in whole Arabidopsis seedlings fed axenically for 24 h with or without (DMSO control) 10 μ M of 4-hydroxybenzoate (4-HB). 4 cl homozygous SALK_043310 (at4g19010) knockout; 2–1: homozygous plants from the T3 generation of RNAi line 2–1. Data are means of four biological replicates \pm SE. Asterisks indicate statistically significant differences from the corresponding wild-type control (i.e., + DMSO or + 4-HB) as determined by Fisher's test (p < α = 0.05) from an analysis of variance.

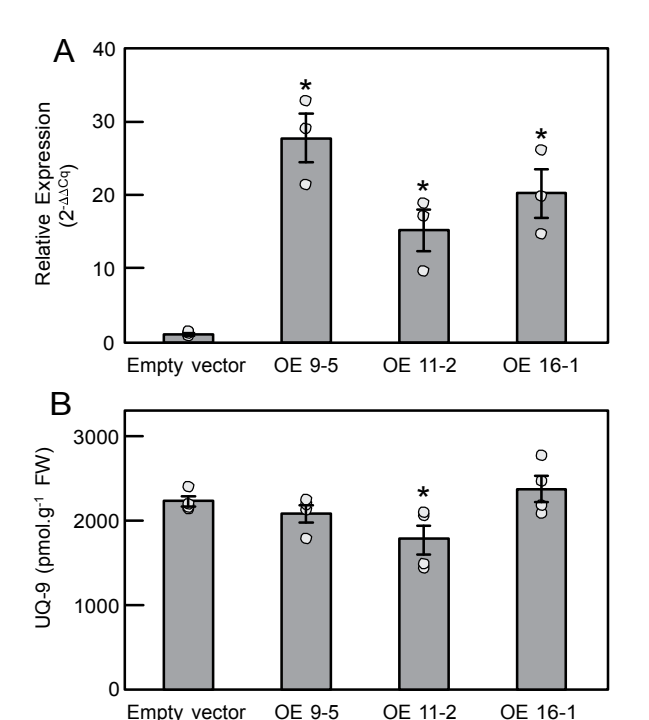


Figure 7. Overexpression of At1g24340. A, qRT-PCR analyses of At1g24340 mRNA levels in the rosette leaves of 4-week-old homozygous T3 plants corresponding to empty vector control and At1g24340-over-expressing transgenics from lines 9–5, 11–2, and 16–1. Each line originates from an independent event of insertion. Data are means of three biological replicates $\pm SE$. Single asterisks indicate significant differences from the empty-vector control as determined by Fisher's test (p < α = 0.05) from an analysis of variance. B, total ubiquinone-9 content in the rosette leaves of 4-week-old homozygous T3 plants corresponding to empty vector control plants and At1g24340-overexpressing transgenics from lines 9–5, 11–2, and 16–1. Data are means of four biological replicates $\pm SE$. Single asterisks indicate significant differences from the empty-vector control as determined by Fisher's test (p < α = 0.05) from an analysis of variance.

function of the fungal homologs is not known, but these enzymes are unlikely to function in ubiquinone biosynthesis either as their harboring species possess Coq7 homologs (Fig. 8A). Phylogenetic reconstructions confirmed that At1g24340, its plant orthologs, and its closest prokaryotic homologs are evolutionarily distinct from UbiF mono-oxygenases, the latter segregating into an outgroup at the root of the At1g24340 phylogeny (Fig. 8C). Remarkably, the plant protein group branches within that of their prokaryotic homologs, forming a sister clade with the hydroxylases acting on halogenated aromatics (Fig. 8C). This arrangement indicates that plant demethoxyubiquinone hydroxylases likely descend from an event of horizontal gene transfer with a bacterium.

Discussion

The C-6 hydroxylation of ubiquinone's ring has long remained elusive in plants, orthologs of the canonical demethoxyubiquinone hydroxylases Coq7 and UbiF missing in all Viridiplantae lineages. In this study, we demonstrate that plant demethoxyubiquinone hydroxylase is structurally and evolutionary distinct from all eukaryotic or prokaryotic ubiquinone

biosynthetic monooxygenases known to date. Phylogenetic reconstructions indicate that the plant enzyme is instead most closely related to bacterial monooxygenases that act on halogenated aromatic compounds. These enzymes belong to group A of FAD-dependent monooxygenases, which are single-gene encoded and use NAD(P)H as an electron donor (37). Most of these monooxygenases act on phenolic compounds, for which they display marked selectivity and regioselectivity (37). The ubiquinone biosynthetic monooxygenases, UbiF/UbiH/UbiI/ COQ6, are also classified as group A FAD-dependent monooxygenases (23), but lack the conserved C-terminal domain (rv200 residues) of plant demethoxyubiquinone hydroxylase. The function of this domain, which is found in a number of group A FAD-dependent monooxygenases, is uncertain. Structural studies of some bacterial monooxygenases indicate that this domain is localized at the interface of dimers of these enzymes and therefore could take part in their oligomerization (38, 39). However, other group A monooxygenases that harbor a similar C-terminal domain have been shown to be active as monomers (40, 41). The sole consensus seems to be that this C-terminal extension does not contribute directly to the binding of substrates or flavin cofactor (39, 40, 42).

The taxonomic distribution and phylogeny of At1g24340 and of its orthologs suggest that the ancestor of these genes was captured in green algae via an event of horizontal gene transfer with a bacterium. The neo-functionalization of this gene as a demethoxyubiquinone hydroxylase could have either predated or postdated its transfer from bacteria to green algae. Furthermore, the presence of Coq7 in Glaucophytes and Rhodophytes is consistent with the evolutionary scenario in which this carboxylate-bridged diiron enzyme was the ancestral C-6 hydroxylase in all Archaeplastida and was replaced in Viridiplantae by its horizontally inherited counterpart. This FAD-dependent demethoxyubiquinone hydroxylase was then vertically transmitted throughout embryophyte lineages. Failure of homology searches to detect homologs in Gymnosperms likely results from the limited coverage of the existing genome assemblies in this group. The absence or sporadic distribution of other ubiquinone biosynthetic enzymes in Gymnosperm species strongly supports this possibility (data not shown).

confocal microscopy Laser-scanning shows that GFP-tagged At1g24340 is exclusively targeted to mitochondria, and for that matter is no different from other eukaryotic demethoxyubiquinone hydroxylases (43). Together with 4-hydroxybenzoate prenyltransferase (EC 2.5.1.39; COQ2) and polyprenyldihydroxybenzoate/demethylubiquinone 3-Omethyltransferase (EC 2.1.1.114/2.1.1.64; COQ3) (4, 15, 44), demethoxyubiquinone hydroxylase is therefore the third ring decoration enzyme of the ubiquinone biosynthetic pathway in plants now shown to localize to mitochondria. These results contradict the early report that the prenyl transferase, methyl transferase, and hydroxylase activities associated with ubiquinone biosynthesis in plants copurify with endoplasmic reticulum/Golgi apparatus-containing fractions (45). The recent observations that ubiquinone biosynthetic enzymes

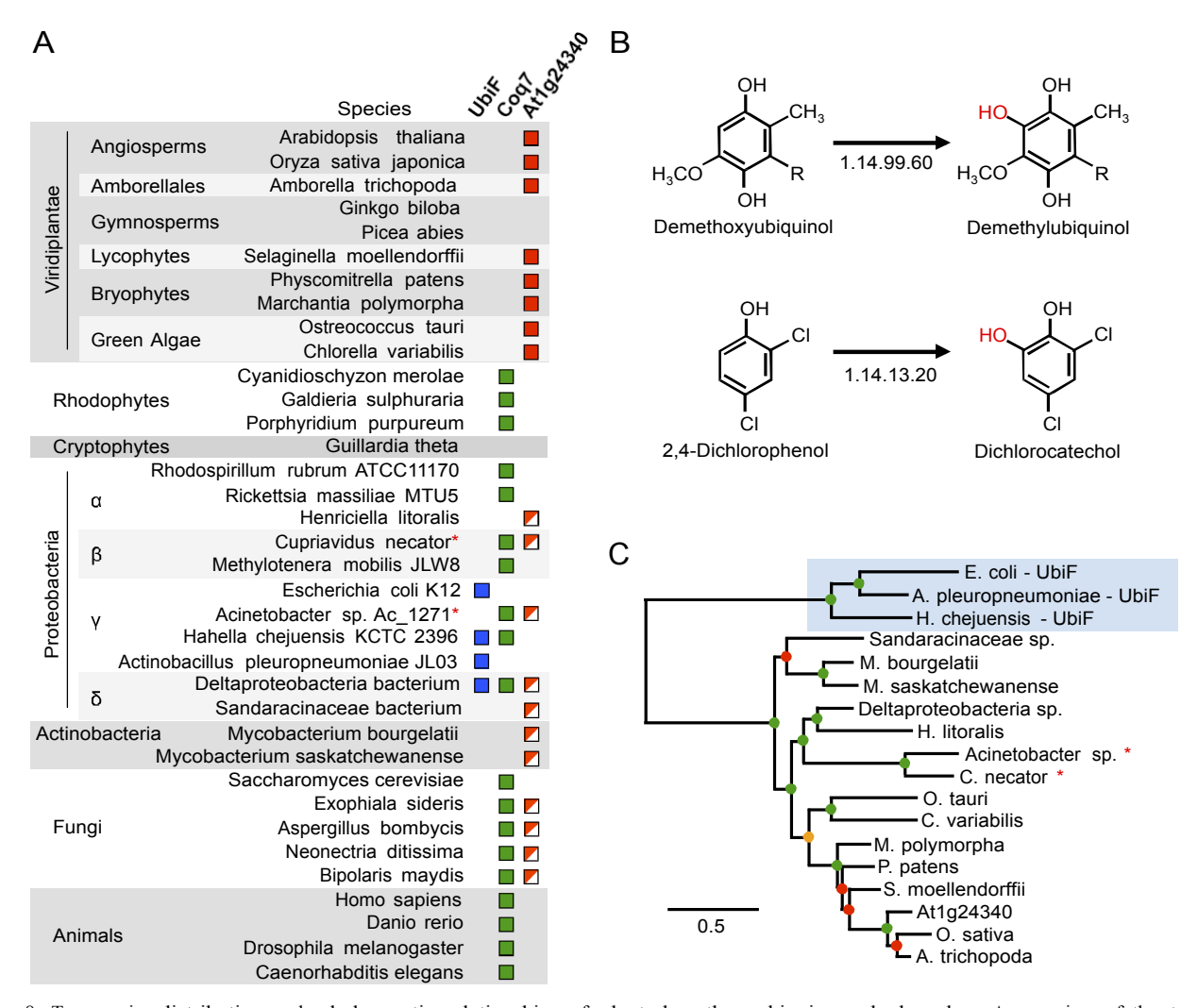


Figure 8. Taxonomic distribution and phylogenetic relationships of plant demethoxyubiquinone hydroxylase. A, overview of the taxonomic occurrence of demethoxyubiquinone hydroxylases and At1g24340 homologs. Red squares indicate At1g24340 orthologs. Red and white squares indicate close homologs of At1g24340 in fungi and bacteria; among those, asterisks indicate 2,4-dichlorophenol hydroxylase (EC 1.14.13.20) that has been shown to function in the catabolism of the halogenated aromatic 2,4-dichlorophenoxyacetic acid. B, substrate regioselectivity of demethoxyubiquinone hydroxylase and 2,4-dichlorophenol hydroxylase. C, maximum likelihood phylogeny of At1g24340 and its closest homologs sampled throughout eukaryotic and prokaryotic lineages. UbiF monoxygenases represent the outgroup. Green, orange, and red dots indicate branch support values ≥70%, ≥50% and <70%, and <50%, respectively. Protein accession numbers are provided in Table S3.

involved in the ring decoration steps associate within discrete mitochondrial domains at the points of contact with the endoplasmic reticulum (46, 47) strongly suggest that subcellular fractionation procedures may shear off such membrane structures, resulting in the artifactual localization of some ubiquinone biosynthetic enzymes in microsomes.

Loss of function of At1g24340 results in embryo lethality, which strongly suggests that the Arabidopsis genome does not encode for additional demethoxyubiquinone hydroxylases. Our data also indicate that overexpression of demethoxyubiquinone hydroxylase alone is not sufficient to boost ubiquinone content in Arabidopsis. This finding is in marked contrast with the situation observed in yeast, in which deregulation of Coq7 activity has been shown to result in a 250% increase in ubiquinone level (18, 48). Last, our functional complementation assays demonstrating that At1g24340 encodes for a strictly monofunctional monooxygenase imply that plants must possess a separate enzyme

for the C-1 hydroxylation step of their ubiquinone biosynthetic pathway.

Experimental procedures

Bioinformatics

Gene networks in Arabidopsis, Medicago truncatula, soybean, rice, and tomato were reconstructed from the top 200 coexpressors of expressed loci mined from the ATTED-II database ((49); https://atted.jp) using At1g24340 as an initial query. Respiratory genes were manually extracted from the resulting lists of coexpressed genes and their functional annotations verified via TAIR (https://www.arabidopsis.org/index.jsp) for Arabidopsis genes and via BLASTp searches for M. truncatula, soybean, rice, and tomato (Dataset S1). Protein domain predictions were performed using the InterPro search tools ((50); http://www.ebi.ac.uk/interpro/). Coordinates for predicted models of At1g24340, E. coli UbiF, and

Saccharomyces cerevisiae COQ7 were retrieved from the AlphaFold Protein Structure Database at EMBL-EBI (https:// alphafold.ebi.ac.uk) (51). Superposition of the At1g24340 and E. coli UbiF models was performed in Coot (52) using secondary structure matching (53). The core superimposed regions of At1g24340 and E. coli UbiF comprise the FAD/ NAD(P)H domains (315 amino acids with 25 gaps) and have a Cα RMSD of 2.95 Å with 16% sequence identity. Visualization of protein models was made with POVScript+ (54). For phylogenetic reconstructions, At1g24340 homologs mined using BLASTp searches (Table S3) and analyzed using the following phylogeny tool suite from Phylogeny.fr (55): MUSCLE for multiple alignments, Gblocks for curation of misalignments and divergent regions, PhyML for maximum likelihood reconstruction, and TreeDyn for tree visualization. Default parameters were used for all the programs.

Chemical and reagents

Standards of ubiquinone-6, -9, and -10 were from Sigma-Aldrich. Ubiquinone-8 was purified from E. coli extracts. Briefly, E. coli cells from a 50-ml aerobic culture were pelleted, washed once with 25 ml of 0.9% (w/v) NaCl solution, and resuspended in 1 ml of water. Cells were transferred to a pyrex screw cap tube containing 500 µl of 0.1 mm zirconia/silica beads (Biospec products) and were vortexed for 90 s. Two milliliters of 95% (v/v) ethanol was then added to the disrupted cells, and the mixture was heated at 70 °C for 10 min. This extract was then partitioned twice with 5 ml of hexane, and the hexane layers were combined and evaporated to dryness using a gentle flow of N2. The sample was resuspended in 1 ml of methanol:dichloromethane (10:1) and chromatographed (100 µl injections) on a 5 µM Supelco Discovery C-18 column (25 cm × 4.6 mm, Sigma-Aldrich) maintained at 30 °C and developed at a flow rate of 1.5 ml min⁻¹ with 100% methanol. Ubiquinone-8 (retention time 17.6 min) was manually collected between 17.4 and 17.8 min by absorbance monitoring at 275 nm, and pooled fractions were evaporated to dryness using a gentle flow of N2. Solutions of ubiquinone standards were prepared in 100% ethanol and quantified using following extinction coefficients at $14,900 \text{ M}^{-1} \text{ cm}^{-1}$ (Q-6 and Q-8), $14,700 \text{ M}^{-1} \text{ cm}^{-1}$ (Q-9), and 14,600 M⁻¹ cm⁻¹ (Q-10) (56). Quinol counterparts were prepared by reaction with sodium borohydride. L-Phe-[ring-¹³C₆] and L-Tyr-[13C₉-15N] were from Cambridge Isotope Laboratories Inc. Unless otherwise mentioned, other chemicals and reagents were from Fisher Scientific.

E. coli and yeast strains

E. coli strain Δ ubiIc (cured) was that described in (26). E. coli strains Δ ubiH (JW2875-1; Δ ubiH758::kan) and Δ ubiF (JW0659-5; Δ ubiF722::kan) were from the Keio collection (57) and were obtained from CGSC (https://cgsc.biology.yale.edu). S. cerevisiae strain E194KCoq7 (MAT α leu2-3112 ura3-52 trp1-289 his4-580 coq7 G580 A (KAN)) and its JM43 parent (MAT α leu2-3112 ura3-52 trp1-289 his4-580) were those described in (28).

Functional complementations of E. coli and yeast mutants

Gene-specific primers for the PCR amplifications described thereafter are listed in Table S2. Full-length and truncated cDNAs of At3g24200 (D50→M50) and At1g24340 (E42→M42) were prepared from Arabidopsis (Col-0) total leaf RNAs using the RNeasy Plant Mini Kit (Qiagen) and RT-PCR. E. coli genes ubiI, ubiH, and ubiF were PCR amplified from E.coli (K12) genomic DNA. Yeast gene COQ7 was PCR amplified from the genomic DNA of S. cerevisiae strain BY4741. PCR products corresponding to the truncated cDNAs of At3g24200 and At1g24340, ubiI, ubiH, and ubiF were cloned into EcoRI/XbaIdigested pBAD24 (58) using In-Fusion Cloning strategy (Takara Bio). PCR products corresponding to the full-length cDNA of At3g24200, At1g24340, and COQ7 were cloned into yeast expression vector pYES-DEST52 using Gateway technologies (Invitrogen). Empty pBAD24 and pYES-DEST52 were used as negative controls of complementation. Yeast transformants were selected at 30 °C on DOB media (MP Biomedicals) + CSM without uracil (MP Biomedicals). Selection medium of the E194KCoq7 strain also contained G418 (200 µg/ml). E. coli transformants were selected using the appropriate antibiotics. For analyses of yeast phenotypes on plates, overnight liquid precultures were diluted at a final optical density of 0.2, 0.02, 0.002, or 0.0002 at 600 nm, and were spotted on YNB solid medium with ammonium sulfate (MP Biodemicals) containing the appropriate amino acids, 2% (w/v) glucose or 3% (v/v) glycerol/2.5% (v/v) ethanol as carbon sources, and 0.05% (w/v) D-galactose as an inducer. Plates were incubated at 30 °C for 2 days (glucose) or 4 days (glycerol/ethanol).

Plant material and growth conditions

Arabidopsis SALK 073461C and SALK 084134 (59) insertion lines were obtained from ABRC (genotyping primers are listed in Table S2). The Arabidopsis 4 cl mutant (SALK 043310) was that described in (12). The three antisense constructs targeting At1g24340 were synthesized (Genscript) based on cDNA base numbering as follows: RNAi-1, 7 to 330 (sense) and 7 to 595 (antisense); RNAi-2, 678 to 980 (sense) and 678 to 1219 (antisense); RNAi-3, 1087 to 1358 (sense) and 1087 to 1608 (antisense). Each construct included 100-bp Gateway cloning sequences attL1 and aatL2 (Invitrogen) at the 5° -end and 3° -end, respectively. These constructs were cloned into pUC57 (Genscript) and then transferred into plant constitutive expression vector pB2GW7 (60) using Gateway technology. The overexpression construct was generated by subcloning full-length At1g24340 cDNA into pB2GW7 using Gateway technology (PCR primers are listed in Table S2). Antisense, overexpression, and vector alone constructs were introduced into Arabidopsis plants (Col-0) via Agrobacterium tumefaciens strain C58C1 using the floral dip method (61). T1 transgenics were selected on soil with glufosinate (120 mg ml⁻¹) applications. Segregating T2 lines were selected on Murashige and Skoog solid medium (MP Biomedicals) containing 1% (w/v) sucrose and glufosinate (20 mg ml⁻¹) and then transferred to soil. The same in vitro selection was used to

determine the germination ratios of T3 plants and identify their homozygous T2 parent lines. For quantitative Real-Time PCR (qRT-PCR) analysis, total RNAs were prepared from rosette leaves using the RNeasy Plant Mini Kit (Qiagen) and quantified by absorbance at 260 nm. cDNAs were synthesized using the ImProm-II Reverse Transcription System (Promega). PCR amplifications were performed using the Applied Biosystems StepOnePlus Real-Time PCR System with PowerUp SYBR Green Master Mix (Applied Biosystems) and the reference gene actin2 (At3g18780) according to the $2^{-\Delta\Delta Cq}$ method. Corresponding PCR primers are listed in Table S2. For both in vitro and soil-grown plants, standard culture conditions were 12-h days (110 μ E m⁻² s⁻¹) at 22 °C, and soil-grown plants were fertilized biweekly. For high light and dark experiments, plants were acclimated to continuous high light intensity (500 µE m⁻² s⁻¹) or continuous darkness for 24 h prior to harvesting the rosette leaves. For heavy isotope feeding experiments, homozygous T2 plants were germinated on Murashige and Skoog solid medium (1% [w/v] sucrose). After 7 days seedlings were transferred to sterile flasks containing 20 ml of Murashige and Skoog medium (1% [w/v] sucrose) with gentle shaking in 12-h days (110 μ E m⁻² s⁻¹) at 22 °C. After 10 to 11 days, 250 μM doses of L-Phe-[ring-¹³C₆] and L-Tyr-[13C₉-15N] were added to the cultures, and whole plants were harvested 3 h later.

Ubiquinone analyses

Yeast cells were cultured at 30 °C in YNB with ammonium sulfate (MP Biomedicals) + CSM without uracil (MP Biomedicals) liquid medium containing 0.1% glucose (w/v) as a carbon source and 2% (w/v) D-galactose as an inducer. E. coli was grown aerobically at 37 °C in LB medium with 0.02 to 0.2% (w/v) or without arabinose as an inducer. Yeast and E. coli cultures (20 ml) were harvested in the mid to late-log phase, and cell pellets were resuspended in 1 ml of water. Cell suspensions were quantified by absorbance at 600 nm and stored at -80 °C. Extractions of yeast cell pellets and Arabidopsis tissues were performed as described in (3). The extraction procedure of E. coli cell pellets was similar to that used for yeast except that the cell disruption step was carried out using 0.1 mm zirconia/silica beads (Biospec products). Ubiquinone-10 (1.5-5.5 nmol) was added to the extracts as an internal standard. Extracts were analyzed by HPLC with diode array detection using a 5 µM Supelco Discovery C-18 column (25 cm × 4.6 mm, Sigma-Aldrich) thermostated at 30 °C. The column eluate was monitored at 275 nm (quinones) and 290 nm (quinols). For yeast samples, the column was developed at a flow rate of 1 ml min⁻¹ in a stepwise fashion with 100% methanol from 0 to 13 min and then 90% methanol/10% hexane from 13 to 42 min. Retention times were 11.4 min (ubiquinone-6) and 28.5 min (ubiquinone-10). Ubiquinol-6 was converted into ubiquinone-6 during the extraction procedure. For E. coli and Arabidopsis samples, the column was developed at a flow rate of 1 ml min⁻¹ in isocratic mode with 90% methanol/10% hexane. Retention times were 9 min (octaprenylphenol), 9.2 min (ubiquinol-9), 9.3

(demethoxyubiquinone-8), 10 min (ubiquinone-8), 12 min (ubiquinol-10), and 17.2 min (ubiquinone-10). Ubiquinol-8 fully reoxidized into ubiquinone-8 during the extraction of the E. coli cells. Data were corrected for recovery, and for Arabidopsis samples reoxidation, of the ubiquinone-10 internal standard. Recovery values ranged from 70% to 95%; quinol reoxidation in Arabidopsis samples was approximately 10%. For UPLC-QTOF analyses, Arabidopsis samples (27–238 mg of fresh weight) were spiked with 100 pmol of ubiquinone-10 and processed as previously described (3) except that the reduction step with NaBH₄ was omitted. Extracts (0.2 ml in methanol:dichloromethane [10:1, vol/vol]) were chromatographed on a Zorbax Eclipse Plus C18 RRHD (50 × 2.1 mm, 1.8 µm, Agilent Technologies) held at 40 °C and at a flow rate of 0.2 ml min⁻¹. Mobile phases consisted of (A) 10 mM ammonium acetate in methanol:isopropanol (80:20, vol/vol) and (B) 10 mM ammonium acetate in isopropanol:hexane (60:40, vol/vol). The column was developed using the following elution program: 15% B (0-3 min), linear gradient 15 to 60% B (3-5 min), 60% B (5-6 min), and 2 min post run reequilibration to initial conditions. The column eluate was analyzed in positive ionization mode using a hybrid quadrupole orthogonal time of flight spectrometer (Agilent Technologies) equipped with a dual Agilent Jet Stream electrospray ionization source. The spectrometer was operated in scan mode (70–2000 m/z) at 3 spectra s⁻¹ with the following source conditions: capillary voltage, 3000 V; nozzle voltage, 2000 V; gas temperature, 200 °C; drying gas flow, 13 ml min⁻¹; nebulizer pressure, 20 psig; sheath gas flow, 12 ml min⁻¹. [¹³C₆]ubiquinone-9 and ubiquinone-9 (retention time 4.72 min) were quantified as [M+NH₄] ammonium adducts at m/z 818.65 and m/z 812.65, respectively. Recovery corrections were performed via quantification of the ammonium adduct of ubiquinone-10 (m/z 880.72; retention time 5.74 min). Quantification of the rate of de novo ubiquinone biosynthesis in continuous high light conditions or continuous dark conditions was performed as described in (14).

Subcellular localization of At1g24340

At1g24340 cDNA was PCR amplified minus its stop codon (primers are listed in Table S2) and cloned into pK7FWG2 (60) using Gateway technology (Invitrogen) resulting in an inframe fusion of At1g24340 to the 5° -end of GFP. This construct was electroporated into A. tumefaciens C58C1, and the transformed cells were coinfiltrated into the abaxial side of the leaves of N. benthamiana together with an A. tumefaciens strain harboring pZP212 for expression of an RFF-tagged fragment of isovaleryl-CoA dehydrogenase (62). Leaves were imaged 48 h later using a Nikon A1 Plus confocal Microscope equipped with a Plan Apo VC 60 × A WI DIC N2 objective. Imaging and analyses were done with Nikon NIS-Elements 5.20.02 (Build 1453). GFP, RFP, and chlorophyll were excited and collected sequentially using the following excitation/emissions wavelengths: 488 nm/500 to 550 nm (GFP), 561 nm/570 to 620 nm (RFP), and 640 nm/650 to 720 nm (chlorophyll).

Data availability

All data are contained within the manuscript.

Supporting information—This article contains supporting information.

Acknowledgments—The authors thank Dr Denise Tieman (University of Florida) for her advice with the silencing strategy, and Dr Fabien Pierrel (University of Grenoble Alpes) for the gift of the E.coli ΔubiIc strain.

Author contributions—S. L., E. S., A. K. B., C. E., A. C., M. A. W., and G. J. B. conceptualization; S. L., S. A. K., L. R. S., A. B., A. C. B., E. S., J. W., C. F. C., A. K. B., T. A. C., C. E., A. C., and G. J. B. data curation; S. L., S. A. K., L. R. S., A. B., A. C. B., E. S., J. W., A. K. B., C. E., A. C., M. A. W., and G. J. B. formal analysis; A. C. B., E. S., C. F. C., A. K. B., T. A. C., A. C., M. A. W., and G. J. B. funding acquisition; S. L., S. A. K., L. R. S., A. B., A. C. B., E. S., J. W., A. K. B., T. A. C., C. E., A. C., and G. J. B. investigation; S. L., S. A. K., L. R. S., A. B., A. C. B., E. S., J. W., C. F. C., A. K. B., T. A. C., C. E., A. C., M. A. W., and G. J. B. methodology; G. J. B. project administration; S. A. K., C. F. C., A. K. B., T. A. C., C. E., A. C., and G. J. B. resources; S. L., C. F. C., A. K. B., T. A. C., C. E., A. C., M. A. W., and G. J. B. supervision; S. L., S. A. K., L. R. S., A. B., A. C. B., E. S., J. W., C. F. C., A. K. B., T. A. C., C. E., A. C., M. A. W., and G. J. B. validation; S. L., S. A. K., L. R. S., A. B., A. C. B., E. S., J. W., C. F. C., A. K. B., T. A. C., C. E., A. C., and G. J. B. visualization; S. L., M. A. W., and G. J. B. writing-original draft; S. L., S. A. K., L. R. S., A. B., A. C. B., E. S., J. W., A. K. B., T. A. C., C. E., A. C. writing-review and editing.

Funding and additional information—This work was made possible in part by National Science Foundation Grants MCB-1712608 (G. J. B.), MCB-1933580 (A. C.), and Graduate Research Fellowship Program DGE-1842473 (A. C. B.), National Institute of Health Grant R01GM139978 (M. A. W.), USDA-ARS Floriculture and Nursery Research Initiative (T. A. C.), and the United States Department of Agriculture-Agriculture Research Service project 6036-11210-001-00D (A. K. B.). The content is solely the responsibility of the authors and does not necessarily represent the official views of the National Institutes of Health.

Conflict of interest—The authors declare that they have no conflicts of interests with the contents of this article.

References

- Bentinger, M., Tekle, M., and Dallner, G. (2010) Coenzyme Q biosynthesis and functions. Biochem. Biophys. Res. Commun. 396, 74

 –79
- Nowicka, B., and Kruk, J. (2010) Occurrence, biosynthesis and function of isoprenoid quinones. Biochim. Biophys. Acta 1797, 1587–1605
- Ducluzeau, A.-L., Wamboldt, Y., Elowsky, C. G., MacKenzie, S. A., Schuurink, R. C., and Basset, G. J. C. (2012) Gene network reconstruction identifies the authentic trans-prenyl diphosphate synthase that makes the solanesyl moiety of ubiquinone-9 in Arabidopsis. Plant J. 69, 366–375
- Okada, K., Ohara, K., Yazaki, K., Nozaki, K., Uchida, N., Kawamukai, M., Nojiri, H., and Yamane, H. (2004) The AtPPT1 gene encoding 4-hydroxybenzoate polyprenyl diphosphate transferase in ubiquinone biosynthesis is required for embryo development in Arabidopsis thaliana. Plant Mol. Biol. 55, 567–577
- Bentinger, M., Brismar, K., and Dallner, G. (2007) The antioxidant role of coenzyme Q. Mitochondrion 7S, S41–S50

- Ohara, K., Kokado, Y., Yamamoto, H., Sato, F., and Yazaki, K. (2004) Engineering of ubiquinone biosynthesis using the yeast coq2 gene confers oxidative stress tolerance in transgenic tobacco. Plant J. 40, 734–743
- Takahashi, S., Ogiyama, Y., Kusano, H., Shimada, H., Kawamukai, M., and Kadowaki, K. (2006) Metabolic engineering of coenzyme Q by modification of isoprenoid side chain in plant. FEBS Lett. 580, 955–959
- Parmar, S. S., Jaiwal, A., Dhankher, O. P., and Jaiwal, P. K. (2015) Coenzyme Q10 production in plants: Current status and future prospects. Crit. Rev. Biotechnol. 35, 152–164
- Liu, M., Chen, X., Wang, M., and Lu, S. (2019) SmPPT, a 4-hydroxybenzoate polyprenyl diphosphate transferase gene involved in ubiquinone biosynthesis, confers salt tolerance in Salvia miltiorrhiza. Plant Cell Rep. 38, 1527–1540
- 10. Soubeyrand, E., Latimer, S., Bernert, A. C., Keene, S. A., Johnson, T. S., Shin, D., Block, A. K., Colquhoun, T. A., Schäffner, A. R., Kim, J., and Basset, G. J. (2021) 3-O-glycosylation of kaempferol restricts the supply of the benzenoid precursor of ubiquinone (coenzyme Q) in Arabidopsis thaliana. Phytochemistry 186, 112738
- Disch, A., Hemmerlin, A., Bach, T. J., and Rohmer, M. (1998) Mevalonate-derived isopentenyl diphosphate is the biosynthetic precursor of ubiquinone prenyl side chain in tobacco BY-2 cells. Biochem. J. 15, 615

 621
- Block, A., Widhalm, J. R., Fatihi, A., Cahoon, R. E., Wamboldt, Y., Elowsky, C., Mackenzie, S. A., Cahoon, E. B., Chapple, C., Dudareva, N., and Basset, G. J. (2014) The origin and biosynthesis of the benzenoid moiety of ubiquinone (coenzyme Q) in arabidopsis. Plant Cell 26, 1938— 1948
- Soubeyrand, E., Johnson, T. S., Latimer, S., Block, A., Kim, J., Colquhoun, T. A., Butelli, E., Martin, C., Wilson, M. A., and Basset, G. J. (2018) The peroxidative cleavage of kaempferol contributes to the biosynthesis of the benzenoid moiety of ubiquinone in plants. Plant Cell 30, 2910–2921
- Soubeyrand, E., Kelly, M., Keene, S. A., Bernert, A. C., Latimer, S., Johnson, T. S., Elowsky, C., Colquhoun, T. A., Block, A. K., and Basset, G. J. (2019) Arabidopsis 4-COUMAROYL-COA LIGASE 8 contributes to the biosynthesis of the benzenoid ring of coenzyme Q in peroxisomes. Biochem. J. 476, 3521–3532
- 15. Avelange-Macherel, M.-H., and Joyard, J. (1998) Cloning and functional expression of AtCOQ3, the Arabidopsis homologue of the yeast COQ3 gene, encoding a methyltransferase from plant mitochondria involved in ubiquinone biosynthesis. Plant J. 14, 203–213
- Hayashi, K., Ogiyama, Y., Yokomi, K., Nakagawa, T., Kaino, T., and Kawamukai, M. (2014) Functional conservation of coenzyme Q biosynthetic genes among yeasts, plants, and humans. PLoS One 9, e99038
- Padilla, S., Tran, U. C., Jiménez-Hidalgo, M., López-Martín, J. M., Martín-Montalvo, A., Clarke, C. F., Navas, P., and Santos-Ocaña, C. (2009) Hydroxylation of demethoxy-Q6 constitutes a control point in yeast coenzyme Q6 biosynthesis. Cell Mol. Life Sci. 66, 173–186
- Martín-Montalvo, A., González-Mariscal, I., Padilla, S., Ballesteros, M., Brautigan, D. L., Navas, P., and Santos-Ocaña, C. (2011) Respiratoryinduced coenzyme Q biosynthesis is regulated by a phosphorylation cycle of Cat5p/Coq7p. Biochem. J. 440, 107–114
- Martín-Montalvo, A., González-Mariscal, I., Pomares-Viciana, T., Padilla-López, S., Ballesteros, M., Vazquez-Fonseca, L., Gandolfo, P., Brautigan, D. L., Navas, P., and Santos-Ocaña, C. (2013) The phosphatase Ptc7 induces coenzyme Q biosynthesis by activating the hydroxylase Coq7 in yeast. J. Biol. Chem. 288, 28126–28137
- Marbois, B. N., and Clarke, C. F. (1996) The COQ7 gene encodes a protein in saccharomyces cerevisiae necessary for ubiquinone biosynthesis. J. Biol. Chem. 271, 2995–3004
- Stenmark, P., Grünler, J., Mattsson, J., Sindelar, P. J., Nordlund, P., and Berthold, D. A. (2001) A new member of the family of di-iron carboxylate proteins. Coq7 (clk-1), a membrane-bound hydroxylase involved in ubiquinone biosynthesis. J. Biol. Chem. 276, 33297–33300
- 22. Behan, R. K., and Lippard, S. J. (2010) The aging-associated enzyme CLK-1 is a member of the carboxylate-bridged diiron family of proteins. Biochemistry 49, 9679–9681
- Pelosi, L., Ducluzeau, A. L., Loiseau, L., Barras, F., Schneider, D., Junier, I., and Pierrel, F. (2016) Evolution of ubiquinone biosynthesis:

- Multiple proteobacterial enzymes with various regioselectivities to catalyze three contiguous aromatic hydroxylation reactions. mSystems 1, e00091-16
- 24. Young, I. G., McCann, L. M., Stroobant, P., and Gibson, F. (1971) Characterization and genetic analysis of mutant strains of Escherichia coli K-12 accumulating the biquinone precursors 2-octaprenyl-6-methoxy-1, 4-benzoquinone and 2-octaprenyl-3-methyl-6-methoxy-1,4benzoquinone. J. Bacteriol. 105, 769–778
- Nakahigashi, K., Miyamoto, K., Nishimura, K., and Inokuchi, H. (1992) Isolation and characterization of a light-sensitive mutant of Escherichia coli K-12 with a mutation in a gene that is required for the biosynthesis of ubiquinone. J. Bacteriol. 174, 7352–7359
- 26. Hajj Chehade, M., Loiseau, L., Lombard, M., Pecqueur, L., Ismail, A., Smadja, M., Golinelli-Pimpaneau, B., Mellot-Draznieks, C., Hamelin, O., Aussel, L., Kieffer-Jaquinod, S., Labessan, N., Barras, F., Fontecave, M., and Pierrel, F. (2013) ubil, a new gene in Escherichia coli coenzyme Q biosynthesis, is involved in aerobic C5-hydroxylation. J. Biol. Chem. 288, 20085–20092
- 27. Pelosi, L., Vo, C. D., Abby, S. S., Loiseau, L., Rascalou, B., Hajj Chehade, M., Faivre, B., Goussé, M., Chenal, C., Touati, N., Binet, L., Cornu, D., Fyfe, C. D., Fontecave, M., Barras, F., et al. (2019) Ubiquinone biosynthesis over the entire O₂ range: Characterization of a conserved O₂-independent pathway. mBio 10, e01319-19
- 28. Tran, U. C., Marbois, B., Gin, P., Gulmezian, M., Jonassen, T., and Clarke, C. F. (2006) Complementation of Saccharomyces cerevisiae coq7 mutants by mitochondrial targeting of the Escherichia coli UbiF polypeptide: Two functions of yeast Coq7 polypeptide in coenzyme Q biosynthesis. J. Biol. Chem. 281, 16401–16409
- Meinke, D. W. (2020) Genome-wide identification of EMBRYO-DEFECTIVE (EMB) genes required for growth and development in Arabidopsis. New Phytol. 226, 306–325
- Meinke, D., Sweeney, C., and Muralla, R. (2009) Integrating the genetic and physical maps of Arabidopsis thaliana: Identification of mapped alleles of cloned essential (EMB) genes. PLoS One 4, e7386
- Almagro Armenteros, J. J., Sønderby, C. K., Sønderby, S. K., Nielsen, H., and Winther, O. (2017) DeepLoc: Prediction of protein subcellular localization using deep learning. Bioinformatics 33, 3387–3395
- Small, I., Peeters, N., Legeai, F., and Lurin, C. (2004) Predotar: A tool for rapidly screening proteomes for N-terminal targeting sequences. Proteomics 4, 1581–1590
- Senkler, J., Senkler, M., Eubel, H., Hildebrandt, T., Lengwenus, C., Schertl, P., Schwarzländer, M., Wagner, S., Wittig, I., and Braun, H. P. (2017) The mitochondrial complexome of Arabidopsis thaliana. Plant J. 89, 1079–1092
- Horton, P., Park, K. J., Obayashi, T., Fujita, N., Harada, H., Adams-Collier, C. J., and Nakai, K. (2007) WoLF PSORT: Protein localization predictor. Nucleic Acids Res. 35, W585–W587
- Perkins, E. J., Gordon, M. P., Caceres, O., and Lurquin, P. F. (1990) Organization and sequence analysis of the 2,4-dichlorophenol hydroxylase and dichlorocatechol oxidative operons of plasmid pJP4. J. Bacteriol. 172, 2351–2359
- Ledger, T., Pieper, D. H., and González, B. (2006) Chlorophenol hydroxylases encoded by plasmid pJP4 differentially contribute to chlorophenoxyacetic acid degradation. Appl. Environ. Microbiol. 72, 2783— 2792
- Huijbers, M. M., Montersino, S., Westphal, A. H., Tischler, D., and van Berkel, W. J. (2014) Flavin dependent monooxygenases. Arch. Biochem. Biophys. 544, 2–17
- Hiromoto, T., Fujiwara, S., Hosokawa, K., and Yamaguchi, H. (2006) Crystal structure of 3-hydroxybenzoate hydroxylase from Comamonas testosteroni has a large tunnel for substrate and oxygen access to the active site. J. Mol. Biol. 364, 878–896
- Manenda, M. S., Picard, M.-È., Zhang, L., Cyr, N., Zhu, X., Barma, J., Pascal, J. M., Couture, M., Zhang, C., and Shi, R. (2020) Structural analyses of the Group A flavin-dependent monooxygenase PieE reveal a sliding FAD cofactor conformation bridging OUT and IN conformations. J. Biol. Chem. 295, 4709–4722

- Ryan, K. S., Howard-Jones, A. R., Hamill, M. J., Elliott, S. J., Walsh, C. T., and Drennan, C. L. (2007) Crystallographic trapping in the rebeccamycin biosynthetic enzyme RebC. Proc. Natl. Acad. Sci. U. S. A. 104, 15311– 15316
- Lindqvist, Y., Koskiniemi, H., Jansson, A., Sandalova, T., Schnell, R., Liu, Z., Mäntsälä, P., Niemi, J., and Schneider, G. (2009) Structural basis for substrate recognition and specificity in aklavinone-11-hydroxylase from rhodomycin biosynthesis. J. Mol. Biol. 393, 966–977
- Liu, L. K., Abdelwahab, H., Martin Del Campo, J. S., Mehra-Chaudhary, R., Sobrado, P., and Tanner, J. J. (2016) The structure of the antibiotic deactivating, N-hydroxylating rifampicin monooxygenase. J. Biol. Chem. 291, 21553–21562
- 43. Tran, U. C., and Clarke, C. F. (2007) Endogenous synthesis of coenzyme Q in eukaryotes. Mitochondrion 7, S62–S71
- 44. Ohara, K., Yamamoto, K., Hamamoto, M., Sasaki, K., and Yazaki, K. (2006) Functional characterization of OsPPT1, which encodes phydroxybenzoate polyprenyltransferase involved in ubiquinone biosynthesis in Oryza sativa. Plant Cell Physiol. 47, 581–590
- Swiezewska, E., Dallner, G., Andersson, B., and Ernster, L. (1993)
 Biosynthesis of ubiquinone and plastoquinone in the endoplasmic reticulum-Golgi membranes of spinach leaves. J. Biol. Chem. 268, 494– 1499
- Eisenberg-Bord, M., Tsui, H. S., Antunes, D., Fernández-Del-Río, L., Bradley, M. C., Dunn, C. D., Nguyen, T. P. T., Rapaport, D., Clarke, C. F., and Schuldiner, M. (2019) The endoplasmic reticulum-mitochondria encounter structure complex coordinates coenzyme Q biosynthesis. Contact. https://doi.org/10.1177/2515256418825409
- Subramanian, K., Jochem, A., Le Vasseur, M., Lewis, S., Paulson, B. R., Reddy, T. R., Russell, J. D., Coon, J. J., Pagliarini, D. J., and Nunnari, J. (2019) Coenzyme Q biosynthetic proteins assemble in a substratedependent manner into domains at ER-mitochondria contacts. J. Cell Biol. 218, 1353–1369
- González-Mariscal, I., Martín-Montalvo, A., Ojeda-González, C., Rodríguez-Eguren, A., Gutiérrez-Ríos, P., Navas, P., and Santos-Ocaña, C. (2017) Balanced CoQ₆ biosynthesis is required for lifespan and mitophagy in yeast. Microb. Cell 4, 38–51
- 49. Obayashi, T., Aoki, Y., Tadaka, S., Kagaya, Y., and Kinoshita, K. (2018) ATTED-II in 2018: A plant coexpression database based on investigation of the statistical property of the mutual rank index. Plant Cell Physiol. 59, e3
- 50. Blum, M., Chang, H. Y., Chuguransky, S., Grego, T., Kandasaamy, S., Mitchell, A., Nuka, G., Paysan-Lafosse, T., Qureshi, M., Raj, S., Richardson, L., Salazar, G. A., Williams, L., Bork, P., Bridge, A., et al. (2021) The InterPro protein families and domains database: 20 years on. Nucleic Acids Res. 49, D344–D354
- Jumper, J., Evans, R., Pritzel, A., Green, T., Figurnov, M., Ronneberger, O., Tunyasuvunakool, K., Bates, R., Žídek, A., Potapenko, A., Bridgland, A., Meyer, C., Kohl, S. A. A., Ballard, A. J., Cowie, A., et al. (2021) Highly accurate protein structure prediction with AlphaFold. Nature 596, 583– 589
- Emsley, P., and Cowtan, K. (2004) Coot: Model-building tools for molecular graphics. Acta Crystallogr. D Biol. Crystallogr. 60, 2126–2132
- 53. Krissinel, E., and Henrick, K. (2004) Secondary-structure matching (SSM), a new tool for fast protein structure alignment in three dimensions. Acta Crystallogr. D Biol. Crystallogr. 60, 2256–2268
- Fenn, T. D., Ringe, D., and Petsko, G. A. (2004) POVScript+: A program for model and data visualization using persistence of vision ray-tracing. J. Appl. Cryst. 24, 946–950
- Dereeper, A., Guignon, V., Blanc, G., Audic, S., Buffet, S., Chevenet, F., Dufayard, J.-F., Guindon, S., Lefort, V., Lescot, M., Claverie, J.-M., and Gascuel, O. (2008) Phylogeny.fr: Robust phylogenetic analysis for the non-specialist. Nucleic Acids Res. 36, W465–W469
- Dawson, R. M. C., Elliot, D. C., Elliot, W. H., and Jones, K. M. (1986) Data for Biochemical Research, 3rd Ed., Oxford University Press, New York, NY
- 57. Baba, T., Ara, T., Hasegawa, M., Takai, Y., Okumura, Y., Baba, M., Datsenko, K. A., Tomita, M., Wanner, B. L., and Mori, H. (2006)

- Construction of Escherichia coli K-12 in-frame, single-gene knockout mutants: The Keio collection. Mol. Syst. Biol. https://doi.org/10.1038/msb4100050
- Guzman, L. M., Belin, D., Carson, M. J., and Beckwith, J. (1995) Tight regulation, modulation, and high-level expression by vectors containing the arabinose PBAD promoter. J. Bacteriol. 177, 4121–4130
- Alonso, J. M., Stepanova, A. N., Leisse, T. J., Kim, C. J., Chen, H., Shinn, P., Stevenson, D. K., Zimmerman, J., Barajas, P., Cheuk, R., Gadrinab, C., Heller, C., Jeske, A., Koesema, E., Meyers, C. C., et al. (2003) Genomewide insertional mutagenesis of Arabidopsis thaliana. Science 301, 653– 657
- Karimi, M., Inzé, D., and Depicker, A. (2002) GATEWAY vectors for Agrobacterium-mediated plant transformation. Trends Plant Sci. 7, 193– 105
- Clough, S. J., and Bent, A. F. (1998) Floral dip: A simplified method for Agrobacterium-mediated transformation of Arabidopsis thaliana. Plant J. 16, 735–743
- 62. Latimer, S., Li, Y., Nguyen, T. T. H., Soubeyrand, E., Fatihi, A., Elowsky, C. G., Block, A., Pichersky, E., and Basset, G. J. (2018) Metabolic reconstructions identify plant 3-methylglutaconyl-CoA hydratase that is crucial for branched-chain amino acid catabolism in mitochondria. Plant J. 95, 358–370



Dr Scott Latimer is a postdoctoral researcher in the Department of Horticultural Sciences at the University of Florida. Dr Latimer's research focuses on identifying hidden reactions and missing enzymes in the metabolism of prenylated quinones in plants. His recent discoveries have contributed to a better understanding of the biosynthesis of ubiquinone and phylloquinone, which function as vital electron carriers for respiration and photosynthesis, respectively.